



30 **Abstract**

31 Dioecy, the presence of separate sexes on distinct individuals, has evolved repeatedly  
32 in multiple plant lineages. However, the specific mechanisms through which sex  
33 systems evolve and their commonalities among plant species remain poorly  
34 understood. With both XY and ZW sex systems, the family Salicaceae provides a  
35 system to uncover the evolutionary forces driving sex chromosome turnovers. In this  
36 study, we performed a genome-wide association study to characterize sex  
37 determination in two *Populus* species, *P. euphratica* and *P. alba*. Our results reveal an  
38 XY system of sex determination on chromosome 14 of *P. euphratica*, and a ZW  
39 system on chromosome 19 of *P. alba*. We further assembled the corresponding sex  
40 determination regions, and found that their sex chromosome turnovers may be driven  
41 by the repeated translocations of a *Helitron*-like transposon. During the translocation,  
42 this factor may have captured partial or intact sequences that are orthologous to a  
43 type-A cytokinin response regulator gene. Based on results from this and other  
44 recently published studies, we hypothesize that this gene may act as a master regulator  
45 of sex determination for the entire family. We propose a general model to explain how  
46 the XY and ZW sex systems in this family can be determined by the same *RR* gene.  
47 Our study provides new insights into the diversification of incipient sex chromosome  
48 in flowering plants by showing how transposition and rearrangement of a single gene  
49 can control sex in both XY and ZW systems.

50

51 **Keywords:** Dioecy, Sex determination, Sex chromosome turnover, Genome, *Populus*

52

## 53 **Introduction**

54 The origin and evolution of dioecy (separate sexes) has long been one of the most  
55 fascinating topics for biologists (Henry et al., 2018; Feng *et al.*, 2020). The presence  
56 of dioecy ensures outcrossing and optimal allocation of reproductive resources for  
57 male and female sexual function, thereby providing them with certain advantages in  
58 fertility, survival and evolution (Bawa, 1980). In flowering plants, dioecy occurs in  
59 only ~6% of all species and has independently evolved thousands of times from  
60 hermaphroditic ancestors (Renner and Ricklefs, 1995; Renner, 2014). Many of these  
61 species have sex determined by a pair of heteromorphic sex chromosomes that differ  
62 in morphology and/or sequence, in the form of male heterogamety (XY system) or  
63 female heterogamety (ZW system) (Ming et al., 2011; Charlesworth, 2016). Theory  
64 predicts that sex chromosomes evolve from ancestral autosomes via successive  
65 mutations in two linked genes with complementary dominance (Charlesworth and  
66 Charlesworth, 1978; Charlesworth, 1991). Subsequently, the suppression of  
67 recombination between these two sex determination genes progressively spreads  
68 along Y or W chromosomes, and permits the accumulation of repetitive elements and  
69 duplication or translocation of genomic fragments, which in turn leads to the  
70 formation of a sex-specific region and finally degeneration of the sex chromosome  
71 (Bergero and Charlesworth, 2009; Charlesworth, 2012; Bachtrog, 2013).  
72 Characterizing the genomic architecture of sex in dioecious species is critical for  
73 understanding the origin of sex chromosomes, especially in their early stage of  
74 evolution.

75 Over the past decade, impressive progress has been made in unraveling the  
76 genetic basis of sex determination in several dioecious plants and the evolutionary  
77 history of their sex chromosomes, including papaya (Wang *et al.*, 2012), persimmon  
78 (Akagi *et al.*, 2014), asparagus (Harkess *et al.*, 2017), strawberry (Tenessen *et al.*,  
79 2018), date palm (Torres *et al.*, 2018) and kiwifruit (Akagi *et al.*, 2018, 2019).  
80 Consistent with the independent origins of sex chromosomes, the sex determination  
81 genes identified in these species differ from each another, although most of them  
82 function in similar hormone response pathways (Feng *et al.*, 2020). In addition, a

83 recent study found that the sex chromosome turnover in strawberries is driven by  
84 repeated translocation of a female-specific sequence (Tenessen *et al.*, 2018). The  
85 combined evidence from these studies demonstrates the high variation of plant sex  
86 determination mechanisms, and so understanding the factors that drive the convergent  
87 evolution of sex chromosomes in plants remains elusive (Zhang *et al.*, 2014).

88 The family Salicaceae provides an excellent system to study the drivers of sex  
89 chromosome evolution. This family includes two sister genera, *Populus* and *Salix*,  
90 which are composed exclusively of dioecious species (Peto, 1938; Zhang *et al.*, 2018;  
91 Li *et al.*, 2019). Previous studies in multiple *Salix* species have consistently mapped  
92 the sex determination regions (SDRs) to chromosome 15, and proposed a ZW system  
93 in which females are the heterogametic sex (Pucholt *et al.*, 2015, 2017; Hou *et al.*,  
94 2015; Chen *et al.*, 2016; Zhou *et al.*, 2018, 2020). However, an XY system was  
95 recently identified on chromosome 7 in *S. nigra* (Sanderson *et al.*, 2020). In  
96 comparison, the SDR has been mapped to multiple locations in different *Populus*  
97 species, indicating a dynamic evolutionary history of the sex chromosomes. The SDR  
98 has been mapped to the proximal telomeric end of chromosome 19 in *P. trichocarpa*  
99 and *P. nigra* (sections *Tacamahaca* and *Aigeiros*) (Gaudet *et al.*, 2007; Yin *et al.*, 2008;  
100 Geraldès *et al.*, 2015), and to a pericentromeric region of chromosome 19 in *P.*  
101 *tremula*, *P. tremuloides* and *P. alba* (section *Populus*) (Pakull *et al.*, 2009, 2014;  
102 Paolucci *et al.*, 2010; Kersten *et al.*, 2014). Most *Populus* species display an XY sex  
103 determination system, but there is some evidence that *P. alba* has a ZW system  
104 (Paolucci *et al.*, 2010). Thus far, the only SDR that has been assembled in *Populus* is  
105 that of *P. trichocarpa* and *P. deltoides*, and it appears to be much smaller than those  
106 observed in *Salix* (Geraldès *et al.*, 2015; Xue *et al.*, 2020). Our recent study on the W  
107 chromosome of *S. purpurea* showed intriguing palindromic structures, in which four  
108 copies of the gene encoding a type A cytokinin response regulator (*RR*) were  
109 identified (Zhou *et al.*, 2020). Interestingly, the ortholog of this gene has also been  
110 reported to be associated with sex in *Populus* from section *Tacamahaca* (Geraldès *et*  
111 *al.*, 2015; Bräutigam *et al.*, 2017; Melnikova *et al.*, 2019), which increases the  
112 possibility that this gene is an excellent candidate for a common sex determination



113 mechanism in the Salicaceae. However, it is still unclear whether this candidate gene  
114 is present in all of these SDRs. Most importantly, how the same gene functions in  
115 both the XY and ZW systems remains elusive. Here, we identify the sex  
116 determination systems of two additional *Populus* species, *P. euphratica* and *P. alba*,  
117 which are from sects. *Turanga* and *Populus* respectively (Wang *et al.*, 2020). We  
118 report their complete SDR assemblies and propose a general model to illustrate the  
119 potentially shared mechanism of sex determination in this family.

120

## 121 **Results**

### 122 **Genome assembly**

123 We have previously reported the assembly of the genomes of a male *P. euphratica*  
124 (Zhang *et al.*, 2020) and a male *P. alba* var. *pyramidalis* (a variety of *P. alba*) (Ma *et*  
125 *al.*, 2019). Here we further sequenced and *de novo* assembled female genomes for  
126 both species using Oxford Nanopore reads. The assembly for the female *P. euphratica*  
127 consists of 1,229 contigs with an N50 of 1.7 Mb and a total size of ~529.0 Mb, while  
128 the female *P. alba* var. *pyramidalis* assembly has 357 contigs with an N50 of 3.08 Mb,  
129 covering a total of ~358.5 Mb (**Table S1**). Both assemblies showed extensive synteny  
130 with their respective male reference genomes, and therefore, based on their syntenic  
131 relationships, the assembled contigs were anchored onto 19 pseudochromosomes  
132 (**Figs. S1 and S2**). The chromosome identities were then assigned by comparison to *P.*  
133 *trichocarpa* (Tuskan *et al.*, 2006).

134

### 135 **XY sex determination on chromosome 14 in *P. euphratica***

136 In order to characterize the sex determination system of *P. euphratica*, we  
137 resequenced the genomes of 30 male and 30 female individuals (**Table S2**) and  
138 performed a genome-wide association study (GWAS). Using the male assembly as the  
139 reference genome, a total of 24,651,023 high-quality single nucleotide polymorphisms  
140 (SNPs) were identified. After Bonferroni correction, we recovered 310 SNPs  
141 significantly associated with sex ( $\alpha < 0.05$ ; **Figs. 1A, S3A and Table S3**). In-depth  
142 analysis found that almost all genotypes (99.99%) of these sex-associated loci are

143 homozygous in females, while 93.57% of the genotypes are heterozygous in males  
144 (**Fig. 1B**). A similar pattern was observed when the sex association analysis was  
145 performed by using the female assembly as the reference genome (**Figs. S3B and S4,**  
146 **and Tables S4 and S5**). These results consistently indicate that an XY system is  
147 involved in sex determination of *P. euphratica*.

148 In addition, we found that the vast majority of the significantly sex-associated  
149 SNPs were located at the proximal end of chromosome 14 (the un-anchored scaffold  
150 '001598F' in male genome was located onto chromosome 14 based on its syntenic  
151 relationship with *P. trichocarpa* genome), while a few other SNPs were present at  
152 chromosomes 7, 9, 12 and 19 (**Figs. 1A, 1B and S4, and Table S5**). We then  
153 attempted to use ultra-long nanopore reads generated from a male individual (**Table**  
154 **S6**) to further reconstruct a new assembly with X and Y haplotypes as separate contigs.  
155 This led to the identification of a contig that was highly similar to the sex-associated  
156 regions and specifically contained Y-linked alleles (**Fig. S5**). The Y-linked region was  
157 further determined by examining the relative depth of coverage when aligning male  
158 versus female resequencing reads against the reference (**Fig. S6**). Based on the  
159 syntenic relationship, the SDR of *P. euphratica* can be mapped to the proximal end of  
160 chromosome 14 and the Y-linked region is about 658 kb in length, corresponding to  
161 ~84 kb on the X chromosome (**Fig. 1C**). We found that two segments spanning 440  
162 kb and 135 kb respectively, are specific to the Y-linked region (**Fig. 1C**), suggesting  
163 the occurrence of significant chromosome divergence between the X and Y  
164 haplotypes, which can be maintained by suppressed recombination.

165 We predicted a total of 37 protein-coding genes in the Y-linked region, many of  
166 which have high similarity with genes on other autosomes and are considered as  
167 translocated genes (**Table S7**). Among these, we found that 9 of the Y-specific genes  
168 were annotated as members of the LONELY GUY (LOG) family, which encodes  
169 cytokinin-activating enzymes that play a dominant role in the maintenance of the  
170 shoot apical meristem and in the establishment of determinate floral meristems  
171 (Kuroha *et al.*, 2009; Tokunaga *et al.*, 2012; Han and Jiao, 2015). Ten genes were  
172 identified in both X and Y haplotypes. A phylogenetic analysis of these genes showed

173 that the X and Y alleles began to diverge after their split with *P. trichocarpa* and *P.*  
174 *alba* (**Figs. 1D and S7**), suggesting that the SDR of *P. euphratica* appears to be  
175 established relatively recently.

176

#### 177 **ZW sex determination on chromosome 19 in *P. alba***

178 We used a similar GWAS strategy for 30 male and 30 female resequenced individuals  
179 to characterize the sex determination system of *P. alba* (**Table S8**). When the male  
180 and female assembly was used as a reference genome, respectively, 173 and 55 SNPs  
181 that were significantly associated with sex were identified (**Figs. 2A, 2B, S8 and S9,**  
182 **and Tables S9-S11**). Most of the sex-associated SNPs are heterozygous in females  
183 and homozygous in males (**Fig. 2B and Table S10**), confirming the ZW sex  
184 determination system in *P. alba*, which was also suggested based on genetic mapping  
185 in a previous study (Paolucci *et al.*, 2010).

186 We found that these sex-associated SNPs are mainly located on a non-terminal  
187 region of chromosome 19 (**Figs. 2A, 2B and S8, and Table S10**). Next, we examined  
188 the female-specific depth profile, combined with the support of ultra-long nanopore  
189 reads (**Table S6**), to delineate the W haplotype of *P. alba* to a region of about 140 kb  
190 on chromosome 19, with a corresponding Z haplotype that is only 33 kb in length  
191 (**Figs. 2C, S10 and S11**). Compared to the Z haplotype and corresponding autosomal  
192 regions of the other Salicaceae species, a specific insertion of 69 kb was observed in  
193 the W haplotype, indicating a recent origin of the SDR in *P. alba*.

194 Sequence annotation predicted 18 protein-coding genes in the W haplotype, six of  
195 which were also found in the Z haplotype (**Table S12**). The high identity of these  
196 alleles between the W and Z haplotype suggests that recombination suppression  
197 occurred very recently (**Fig. 2D**). We further found that the gene encoding  
198 NAC-domain protein, *SOMBRERO* (*SMB*), which has a similar function to the  
199 *VND/NST* transcription factors that regulate secondary cell wall thickening in woody  
200 tissues and maturing anthers of *Arabidopsis* (Mitsuda *et al.*, 2005; Bennett *et al.*,  
201 2010), was expanded from one member in the Z haplotype to three copies in the W  
202 haplotype ('HP2' in **Fig. 2D**). There are 12 genes specific to the W haplotype (**Table**

203 **S12**), including *DM2H* (*DANGEROUS MIX2H*), which encodes a nucleotide-binding  
204 domain and leucine-rich repeat immune receptor protein (Chae *et al.*, 2014); *CCR2*  
205 (Cinnamoyl CoA reductase), which is involved in lignin biosynthesis and plant  
206 development (Thevenin *et al.*, 2011); and *STRS1* (*STRESS RESPONSE*  
207 *SUPPRESSORI*), a gene encoding a DEAD-box RNA helicase, which is involved in  
208 epigenetic gene silencing related to stress responses (Khan *et al.*, 2014). More  
209 interesting, we also identified three copies of the gene encoding a type A cytokinin  
210 response regulator (*RR*) in the W-specific region (**Fig. 3A**), the ortholog of which has  
211 also been identified to be associated with sex determination in poplar and willow  
212 (Geraldès *et al.*, 2015; Bräutigam *et al.*, 2017; Melnikova *et al.*, 2019; Zhou *et al.*,  
213 2020). Very little sequence differences were found among these three copies, and  
214 combined with the fact that the ortholog of the *RR* gene is located at the distal end of  
215 chromosome 19 in *P. trichocarpa* and *P. euphratica* (**Fig. 3**), we conclude that the *RR*  
216 gene was translocated from the end of chromosome 19 to the W haplotype of *P. alba*  
217 and then underwent at least two rounds of recent duplication.

218

### 219 **Evidence for SDR turnover in Salicaceae**

220 We have shown that *P. euphratica* and *P. alba* have different sex determination  
221 systems, and that the SDRs are different from those reported in *P. trichocarpa* and *S.*  
222 *purpurea*, indicating extraordinarily high diversity of sex determination in the  
223 Salicaceae. In order to examine whether the sex determination regions originated  
224 independently in each lineage, or evolved into the current SDRs separately after a  
225 common ancient origin, we performed syntenic analysis on these SDRs in *P.*  
226 *euphratica* and *P. alba*, and the corresponding autosomal regions in *P. trichocarpa*  
227 and *S. purpurea*. We found that although the pseudo-autosomal regions of these sex  
228 chromosomes are highly collinear with their corresponding autosomal regions in other  
229 species, the sequences in the sex-specific regions are not alignable (**Figs. 1C and 2C**).  
230 In contrast, although there was little collinearity among these SDRs, a homologous  
231 sequence with multiple duplicates was identified between the Y haplotype of *P.*  
232 *euphratica* and the W haplotype of *P. alba* (**Fig. 3A**). Interestingly, the locations of

233 the duplicates overlapped with the three predicted *RR* genes in *P. alba*. In the  
234 corresponding regions of the Y haplotype of *P. euphratica*, we identified 10 partial  
235 duplicates of the *RR* gene including four covering the first three exons (large  
236 duplicate) and six covering only the first exon (small duplicate) of the *RR* gene (**Fig.**  
237 **3**). Phylogenetic analysis of these duplicates showed that the three *RR* genes in *P.*  
238 *alba* clustered together and are closely related to the intact orthologs of *P. euphratica*  
239 and *P. trichocarpa*, while the partial duplicates from *P. euphratica* divided into two  
240 main clades, one with only large duplicates and a second clade with only small  
241 duplicates (**Fig. 3B**).

242 Since the *RR* duplicates were found in the SDRs of all of the current and  
243 previously studied species, we believe that they may play important roles in sex  
244 determination of the Salicaceae species. These results also lead to the hypothesis that  
245 these species shared an ancient origin of sex chromosomes, followed by frequent  
246 turnover events due to translocation of the *RR* duplicates. This is further supported by  
247 the distant relationship between the partial and intact *RR* duplicates (**Fig. 3B**), which  
248 indicate that the partial duplicates originated before the divergence of these poplar  
249 species and were repeatedly inserted into the SDRs of *P. euphratica*. We did not  
250 detect any structurally intact long terminal repeat retrotransposons (LTR-RTs) around  
251 these *RR* duplicates, which made it impossible to estimate their insertion time.  
252 However, around the *RR* duplicates in *P. euphratica*, we identified a *Helitron*-like  
253 transposable element upstream of each small duplicate except the second one  
254 ('PeuY:S2'), and a *Copia*-like LTR fragment in the downstream region of each large  
255 duplicate (**Fig. 3B**). These two repetitive elements were also identified in all three *RR*  
256 duplicates of *P. alba*, and are located upstream and in the third intron of the *RR* gene,  
257 respectively, similar to that in *P. euphratica*. The phylogenetic trees of the two  
258 elements and the *RR* duplicates exhibited a similar topological relationship,  
259 suggesting that they may be transposed together as a unit (**Figs. 3C and 3D**). The  
260 extremely high similarity of these sequences indicates that they were recently  
261 transposed into the SDRs of *P. euphratica* and *P. alba*, respectively, consistent with  
262 the observation that their sex chromosomes have not been severely degenerated. In

263 addition, we found that the *Helitron*-like element was not present in the upstream  
264 region of the intact *RR* genes at chromosome 19 of *P. euphratica* and *P. trichocarpa*  
265 (**Fig. 3B**), which led us to speculate that this element may be the main driving force  
266 for gene replication during the evolution of SDRs in *P. euphratica* and *P. alba*.  
267 However, we failed to detect the same pattern in *S. purpurea*, in which multiple *Copia*  
268 LTR-RTs were predicted instead of the *Helitron* elements (Zhou *et al.*, 2020). This  
269 implies that poplar and willow may have different SDR turnover mechanisms, which  
270 requires further evidence from more species to confirm.

271

## 272 **Discussion**

273 It is notoriously difficult to assemble the complete sequence of SDRs or sex  
274 chromosomes, which usually have a high repeat density and many translocated  
275 segments from autosomes (Charlesworth, 2012; Bachtrog, 2013). In our study, the  
276 sex-associated loci were initially mapped onto multiple different chromosomes (**Figs.**  
277 **1 and 2**), although they consistently revealed an XY sex determination system in *P.*  
278 *euphratica* and a ZW system in *P. alba*. These results may be caused by the lack  
279 and/or mis-assembly of SDRs in the reference genome, especially when the genome  
280 from a homozygous (XX or ZZ) individual was used as reference, the reads from Y-  
281 or W-specific regions of hemizygous (XY or ZW) individuals may be misaligned to  
282 homologous sequences on autosomes and led to false associations. Similar  
283 phenomena were also observed in the sex association analysis of *P. trichocarpa*, *P.*  
284 *balsamifera* and *S. purpurea*, which may lead to an inaccurate localization of SDRs in  
285 assemblies (Gerald *et al.*, 2015; Zhou *et al.*, 2020). The high sequence similarity  
286 between these sex-associated regions and the SDRs we finally established strongly  
287 supports this possibility (**Figs. S5 and S10**). Therefore, our research emphasizes the  
288 importance and necessity for precise assembly of SDRs using multiple  
289 complementary methods, including the ultra-long read sequencing, haplotype phased  
290 assembly and the sex-specific depth of read mapping.

291 Our results further indicate that the SDRs of poplar species are generally shorter  
292 in length and contain relatively fewer genes than that recently reported in *S. purpurea*

293 (Zhou *et al.*, 2020), though the size of this SDR may be inflated due to overlap with  
294 the centromere (Zhou *et al.*, 2018). Although some specific insertions were observed  
295 on the Y and W chromosomes, we found no obvious degeneration of sex  
296 chromosomes at least in *P. euphratica* and *P. alba*. These results suggest that the  
297 SDRs of these two species were established relatively recently, which is a common  
298 feature of the sex chromosomes of the Salicaceae species studied so far (Geraldes *et*  
299 *al.*, 2015; Pucholt *et al.*, 2017; Zhou *et al.*, 2018, 2020). Along with this, our results  
300 also suggest that the Y and W chromosomes have expanded in content, a pattern that  
301 is common in young sex chromosomes of plants (Hobza *et al.*, 2015, 2017). Moreover,  
302 our results simultaneously showed that the Salicaceae exhibit an extremely fast rate of  
303 sex-chromosome turnover. In previous studies, SDRs have been reported only on  
304 chromosome 15 with female heterogamety (ZW) in willow except *S. nigra* (Pucholt *et*  
305 *al.*, 2015, 2017; Hou *et al.*, 2015; Chen *et al.*, 2016; Zhou *et al.*, 2018, 2020;  
306 Sanderson *et al.*, 2020), and on chromosome 19 of poplar with most species showing  
307 male heterogamety (XY) (Gaudet *et al.*, 2007; Yin *et al.*, 2008; Pakull *et al.*, 2014;  
308 Geraldes *et al.*, 2015). However, our study identified an XY system with the SDR on  
309 chromosome 14 of *P. euphratica* for the first time, and confirmed a ZW system with  
310 SDR on chromosome 19 of *P. alba*. These results highlight the complexity and  
311 diversity of sex determination in this family. Comparative analysis showed that  
312 translocation of genes from autosomes to the SDR and gene replication frequently  
313 occurred both on the Y chromosomes of *P. euphratica* and on the W chromosomes of  
314 *P. alba*, indicating that these two events are likely to be important contributors during  
315 SDR turnover. The regulatory mechanisms and functions of these genes in sex  
316 determination and sexual dimorphism in these two species need further investigation.

317       Among all genes on SDRs, the cytokinin response regulator is the most likely  
318 candidate for controlling sex determination in the Salicaceae, not only because the  
319 orthologs of this gene have been found to be sex-associated in most of the reported  
320 species in the family, but also because it is the only homologous sequence found in  
321 the sex chromosomes of *P. euphratica*, *P. alba*, *P. trichocarpa*, *P. deltoides* and *S.*  
322 *purpurea* (**Fig. 3**), the only Salicaceae species with SDR precisely assembled (Zhou *et*



323 *al.*, 2020; Xue *et al.*, 2020). Recent progress has revealed that the genes involved in  
324 cytokinin signaling play important roles in the regulation of unisexual flower  
325 development in plants (Wybouw *et al.*, 2019; Kieber *et al.*, 2018; Feng *et al.*, 2020).  
326 Specifically, a Y-specific type-C cytokinin response regulator (*Shy Girl*, *SyGI*) was  
327 recently identified as a suppressor of carpel development and therefore is a strong  
328 candidate of sex determination in kiwifruit (Akagi *et al.*, 2018). Similar to the pattern  
329 of the *RR* genes found in the Salicaceae species, in kiwifruit *SyGI* was duplicated  
330 from an autosome and subsequently gained a new function on its Y chromosome.  
331 However, the type-A *RR* genes we identified here are not orthologous to the *SyGI*  
332 gene, so we speculate that they may have different functions in the cytokinin signaling  
333 pathway. Based on our results, it is reasonable to suspect that the *RR* genes are more  
334 likely to function as a dominate promoter of female function (**Fig. 4**), as they exist on  
335 the W chromosomes of both *P. alba* and *S. purpurea* in intact duplicates. In contrast,  
336 the *RR* gene fragments on the Y chromosome of *P. euphratica* exist as two partial  
337 duplicates with different sizes. This may serve as a female suppressor by encoding an  
338 siRNA that targets the intact *RR* gene at the distal end of chromosome 19, possibly  
339 through RNA-directed DNA methylation (Brautigam *et al.*, 2017; Xue *et al.*, 2020). It  
340 should be noted that, although the intact *RR* gene has been reported to be associated  
341 with sex in *P. trichocarpa*, there is still no evidence to support the gene's localization  
342 on its Y chromosome. In the previous GWAS study (Geraldes *et al.*, 2015), most of  
343 the sex-associated loci of *P. trichocarpa* were located on the proximal end of  
344 chromosome 19. The associated signals scattered around the intact *RR* gene, which is  
345 located at the distal end of chromosome 19, were most likely due to assembly errors  
346 arising from the fact that this reference genome is derived from a female (XX)  
347 individual (the major factor in misleading SDR localization as mentioned above).  
348 Therefore, our findings consistently showed that Salicaceae species potentially share a  
349 common mechanism of sex determination, in which the specific duplication of the *RR*  
350 orthologs on SDRs may have played an important role in the acquisition of separate  
351 sexes in these species.

352 More interestingly, we identified *Helitron*-like repetitive elements upstream of the



353 *RR* duplicate in both SDRs of *P. euphratica* and *P. alba*, regardless of whether the *RR*  
354 duplicate is intact or partial (**Fig. 3**). As a major class of DNA transposons, *Helitrons*  
355 were hypothesized to transpose by a rolling circle replication mechanism, and have  
356 been found to frequently capture genes or gene fragments and move them around the  
357 genome, which is believed to be important in the evolution of host genomes  
358 (Morgante *et al.*, 2005; Kapitonov and Jurka, 2007). Our results suggest that the *RR*  
359 fragments and intact gene sequences appear to have been captured by *Helitrons* in *P.*  
360 *euphratica* and *P. alba*, and subsequently replicated in their SDRs (**Figs. 3 and 4**).  
361 Furthermore, our phylogenetic analysis indicated that the intact *RR* gene was captured  
362 very recently in *P. alba*, at least after its split with *P. trichocarpa* (**Fig. 3B**). In contrast,  
363 although we found high similarity among the *RR* partial duplicates of *P. euphratica*,  
364 these sequences are quite different from the intact *RR* genes of other poplar species  
365 (**Fig. 3B**). These results indicate that the partial duplicates were present before the  
366 diversification of poplar species, but only recently replicated on the Y chromosome of  
367 *P. euphratica*. We found that the partial duplicate of the *RR* gene is lacking in *P. alba*,  
368 which may be another key event in addition to the duplication of the intact *RR* gene,  
369 in the transition of the sex determination system from XY to ZW (**Fig. 4**). In addition,  
370 the high nucleotide identity among intact *RR* genes of *S. purpurea* reflects another  
371 possible SDR turnover event in willow, which might be driven by the replication of a  
372 *Copia* LTR (Zhou *et al.*, 2020), rather than by a *Helitron* as we found in poplar.  
373 Moreover, we also identified an inverted repeat of the first exon of the *RR* gene and an  
374 intact copy on the chromosomes 15Z and 19 of *S. purpurea*, respectively (**Fig. 3**).  
375 This suggests a model whereby the inverted repeat is suppressing the *RR* gene of  
376 chromosome 19 in males, but the SDR on the W chromosome may be dominant to  
377 this effect in females, possibly due to increased dosage or another mechanism (**Fig. 4**).  
378 These observations further indicate that the sex determination system of *S. purpurea*  
379 may have been changed from XY to ZW relatively recently, since the suppressing  
380 mechanism from the *RR* partial duplication is still retained. This turnover was also  
381 supported by the XY sex determination system of the basal *Salix* species, *S. nigra*  
382 (Sanderson *et al.*, 2020). Therefore, our results suggest that the high activity of these

383 repetitive elements is the most likely cause of the recently established SDRs in these  
384 species, and further indicate that at least three turnover events have occurred in the  
385 evolution of sex chromosomes of the Salicaceae species (**Fig. 4**).

386 In conclusion, here we present an XY system of sex determination with the SDR  
387 on the proximal end of chromosome 14 in *P. euphratica*, and a ZW system with the  
388 SDR on a non-terminal region of chromosome 19 in *P. alba*. Both SDRs appear to  
389 have evolved relatively recently and are characterized by frequent translocations from  
390 autosomes and gene replication events. Our comparative analysis also demonstrated  
391 an extremely fast rate of sex chromosome turnover among Salicaceae species, which  
392 may be driven by *Helitron* transposons in poplar and by *Copia* LTRs in willow. Most  
393 importantly, we propose a model showing that poplar and willow have a common  
394 underlying mechanism of sex determination, which controls the XY and ZW systems  
395 simultaneously through a type-A *RR* gene. In the future, it will be necessary to  
396 conduct transgenic function experiments and comparative analysis from more species  
397 in this family to further support our model.

398

## 399 **Methods**

### 400 **Genome sequencing**

401 We have previously reported the reference genome of a male *P. euphratica* (Zhang *et*  
402 *al.*, 2020) and a male *P. alba* (Ma *et al.*, 2019). In this study, we further collected the  
403 fresh leaves of a female *P. euphratica* and a female *P. alba* for genome sequencing  
404 and assembly. Genomic DNA was extracted using the QIAGEN Genomic DNA  
405 extraction kit (Qiagen, Hilden, Germany) following the manufacturer's protocol. To  
406 generate Oxford Nanopore long reads, approximately 15 µg of genomic DNA was  
407 size-selected using the BluePippin system (Sage Science, USA), and processed  
408 according to the protocol of Ligation Sequencing Kit (SQK-LSK109). The final  
409 library was sequenced on a PromethION sequencer (Oxford Nanopore Technologies,  
410 UK) with a running time of 48 hours. The Oxford Nanopore proprietary base-caller,  
411 Albacore v2.1.3, was used to perform base calling of the raw signal data and convert  
412 the FAST5 files into FASTQ files.

413 In addition, paired-end libraries with insert size of ~300 bp were also constructed  
414 using NEB Next® Ultra DNA Library Prep Kit (NEB, USA), with the standard  
415 protocol provided by Illumina (San Diego, CA, USA). The library was sequenced on  
416 an Illumina HiSeq X Ten platform (Illumina, San Diego, CA, USA). These  
417 sequencing data were used for correction of errors inherent to long read data for  
418 genome assembly.

419

## 420 **Genome Assembly**

421 For genome assembly, we first removed the Nanopore long reads shorter than 1 kb  
422 and the low-quality reads with a mean quality  $\leq 7$ . The long reads underwent  
423 self-correction using the module 'NextCorrect' and then assembled into contigs using  
424 'NextGraph' implemented in Nextdenovo v2.2.0  
425 (<https://github.com/Nextomics/NextDenovo>) with default parameters. Subsequently,  
426 the filtered Nanopore reads were mapped to the initial assembly using the program  
427 Minimap2 v2.17-r941 (Li, 2018) and NextPolish v1.0  
428 (<https://github.com/Nextomics/NextPolish>) was used with three iterations to polish  
429 the genome. In addition, we further aligned the Illumina reads to the genome using  
430 BWA-MEM v0.7.15 (Li and Durbin 2009) and corrected base-calling by an additional  
431 three rounds of NextPolish runs with default parameters. Finally, the corrected  
432 genome was aligned to their respective male reference genome using the LAST  
433 program (Kielbasa *et al.*, 2011) and the syntenic relationships were used to anchor the  
434 assembled contigs onto 19 chromosomes.

435

## 436 **Population sample collection, resequencing and mapping**

437 Silica gel dried leaves of *P. euphratica* and *P. alba* were collected from wild  
438 populations in western China. For each species, the sex of 30 male and 30 female  
439 individuals was identified from flowering catkins. Genomic DNA of each sample was  
440 extracted using the Qiagen DNeasy Plant Minikit (Qiagen, Hilden, Germany).  
441 Paired-end libraries were prepared using the NEBNext Ultra DNA Library Prep Kit  
442 (NEB, USA) and sequenced on an Illumina HiSeq X Ten platform, according to the

443 manufacturer's instructions.

444 The generated raw reads were first subjected to quality control and low-quality  
445 reads were removed if they met either of the following criteria (Ma *et al.*, 2018): i)  
446  $\geq 10\%$  unidentified nucleotides (N); ii) a phred quality  $\leq 7$  for  $> 65\%$  of read length;  
447 iii) reads overlapping more than 10 bp with the adapter sequence, allowing  $< 2$  bp  
448 mismatch. Reads shorter than 45 bp after trimming were also discarded. The obtained  
449 high-quality cleaned reads were subsequently mapped to the male and female  
450 reference genomes of each species, respectively, using BWA-MEM v0.7.15 with  
451 default parameters (Li and Durbin 2009). Then the alignment results and marked  
452 duplicate reads were sorted using SAMtools v0.1.19 (Li *et al.*, 2009). Finally,  
453 Genome Analysis Toolkit (GATK) (DePristo *et al.*, 2011) was performed to process  
454 base quality recalibrations to enhance alignments in regions around putative indels  
455 with two steps: i) 'RealignerTargetCreator' was applied to identify regions where  
456 realignment was needed; ii) 'IndelRealigner' was used to realign these regions.

457

#### 458 **SNP calling, filtering and genome-wide association study (GWAS)**

459 To prevent biases in SNP calling accuracy due to the difference of samples size  
460 between groups, single-sample SNP and genotype calling were first implemented  
461 using GATK (DePristo *et al.*, 2011) with 'HaplotypeCaller', and then multi-sample  
462 SNPs were identified after merging the results of each individual by  
463 'GenotypeGVCFs'. A series of filtering steps were performed to reduce false  
464 positives (Yang *et al.*, 2018), including removal of (1) indels with a quality scores  $<$   
465 30, (2) SNPs with more than two alleles, (3) SNPs at or within 5 bp from any indels,  
466 (4) SNPs with a genotyping quality scores (GQ)  $< 10$ , and (5) SNPs with extremely  
467 low ( $<$  one-third average depth) or extremely high ( $>$  threefold average depth)  
468 coverage. The identified SNPs were used for subsequent GWAS analysis. A standard  
469 case/control model between allele frequencies and sex phenotype was performed  
470 using Plink v1.9 (Purcell *et al.*, 2007). For each species, associations at  $\alpha < 0.05$  after  
471 Bonferroni correction for multiple testing were reported as the significantly

472 sex-associated SNPs. These sex-associated SNPs that occurred within 10 kb on the  
473 same chromosome were merged into the same interval.

474

#### 475 **Construction of *P. euphratica* Y contig and *P. alba* W contig**

476 To construct the Y contig of *P. euphratica* and the W contig of *P. alba*, we further  
477 generated ultra-long sequences from a male (XY) *P. euphratica* and a female (ZW) *P.*  
478 *alba*, using an optimized DNA extraction followed by modified library preparation  
479 based on the Nanopore PromethION sequencer (Jain *et al.*, 2018; Gong *et al.*, 2019).  
480 For *P. euphratica*, we did not find contigs that clearly contained Y-linked sequences  
481 in its male genome, which may be due to assembly errors, so we used multiple  
482 methods to determine its Y contig. At first, we attempted to find the male-specific  
483 k-mers from the high-quality resequencing reads of both male and female samples.  
484 Briefly, all 32 bp k-mers starting with the ‘AG’ dinucleotide were extracted from all  
485 resequencing reads, and the number of occurrences of each specific subsequence in  
486 female and male individuals was counted, respectively. The use of the ‘AG’  
487 dinucleotide is to reduce the number of k-mer sequences and effectively speed up the  
488 analysis. The k-mer counts were then compared between male and female, and the  
489 male-specific k-mers (female count was 0) were obtained. Next, we extracted the  
490 ultra-long nanopore reads containing at least one of the identified male-specific  
491 k-mers, and assembled these ultra-long reads using the software Canu v1.7 (Koren *et*  
492 *al.*, 2017), resulting in a ‘male-specific contig’ that was 450 kb in length.  
493 Simultaneously, we also *de novo* assembled all of the ultra-long nanopore reads into a  
494 draft male genome using Nextdenovo v2.2.0. By comparing the ‘male-specific contig’  
495 with the obtained male genome, we identified a candidate Y contig that contained a  
496 large number of male-specific alleles and exhibited a widespread synteny and  
497 continuity with the ‘male-specific contig’. To further refine the sex determination  
498 region along this candidate Y contig, we re-mapped the resequencing data to the draft  
499 genome by BWA-MEM v0.7.15 (Li and Durbin, 2009), and extracted the average  
500 depth of coverage using a non-overlapping sliding window (1 kb in length) by  
501 SAMtools v0.1.19 (Li *et al.*, 2009). Finally, we compared the relative depth of

502 coverage between male and female individuals, and found that the region between 0  
503 and 658 kb of this contig showed male-specific depth and was therefore considered to  
504 be the sex determination region on the Y chromosome of *P. euphratica*.

505 For *P. alba*, we first performed a whole genome alignment between its male and  
506 female genome using the program LAST (Kielbasa *et al.*, 2011). Fortunately, we  
507 found that the sex-associated region in the female genome contained a large insert  
508 compared to the corresponding region in the male genome. We used the same method  
509 as above to count the relative depth of coverage between male and female individuals  
510 of *P. alba*, and found that the region between 310 and 450 kb of this contig exhibited  
511 female-specific depth. Therefore, this region was directly considered to be the sex  
512 determination region on the W chromosome of *P. alba*, and the assembly accuracy of  
513 this region was also confirmed by our ultra-long nanopore reads.

#### 514 **Annotation and comparison of the Y and W contigs**

515 Transposable elements in our assembled Y and W contigs were identified and  
516 classified using the software RepeatMasker (Tarailo-Graovac and Chen, 2009). Gene  
517 annotation was conducted by combining the results of *de novo* prediction from the  
518 program Augustus v.3.2.1 (Stanke *et al.*, 2006), homology-based prediction using the  
519 protein sequences of *A. thaliana*, *P. trichocarpa* and *S. purpurea* downloaded from  
520 Phytozome 12 (<https://phytozome.jgi.doe.gov/>), as well as transcriptome data of *P.*  
521 *euphratica* and *P. alba* generated from our previously studies (Ma *et al.*, 2019; Hu *et*  
522 *al.*, 2020; Zhang *et al.*, 2020). The predicted genes were searched against predicted  
523 proteins from *P. trichocarpa*, *S. suchowensis* and *A. thaliana* to find the closest  
524 homologous annotation.

525 To construct the phylogenetic relationships among the allelic genes on the X/Y or  
526 Z/W contigs, we further identified their orthologous genes in *P. pruinosa* (Yang *et al.*,  
527 2017), *P. ilicifolia* (Chen *et al.*, 2020) and *S. suchowensis* (Dai *et al.*, 2014) genomes  
528 by combining reciprocal blast results and their syntenic relationships. The sequences  
529 were aligned using ClustalW with default parameters provided in MEGA5 (Tamura *et*  
530 *al.*, 2011) and the resulting alignments were adjusted manually. A maximum  
531 likelihood tree was built using MEGA5 with default parameters.

532

533 **Accession numbers**

534 The whole genome sequence data reported in this paper have been deposited in the  
535 Genome Warehouse in BIG Data Center (BIG Data Center Members, 2019), Beijing  
536 Institute of Genomics (BIG), Chinese Academy of Sciences, under accession number  
537 PRJCA002485 that is publicly accessible at <https://bigd.big.ac.cn/bioproject>.

538

539 **Acknowledgements**

540 This research was supported by National Natural Science Foundation of China  
541 (31561123001, 31922061, 41871044, 31500502), NSF Dimensions of Biodiversity  
542 Program (1542509 to S.D. and 1542599 to M.O.), National Key Research and  
543 Development Program of China (2016YFD0600101), Fundamental Research Funds  
544 for the Central Universities (SCU2019D013).



545 **References**

- 546 Akagi, T., Henry, I.M., Ohtani, H., Morimoto, T., Beppu, K., Kataoka, I., and Tao, R.  
547 (2018). A Y-Encoded Suppressor of Feminization Arose via Lineage-Specific  
548 Duplication of a Cytokinin Response Regulator in Kiwifruit. *The Plant cell*  
549 30:780-795.
- 550 Akagi, T., Henry, I.M., Tao, R., and Comai, L. (2014). Plant genetics. A  
551 Y-chromosome-encoded small RNA acts as a sex determinant in persimmons.  
552 *Science* 346:646-650.
- 553 Akagi, T., Pilkington, S.M., Varkonyi-Gasic, E., Henry, I.M., Sugano, S.S., Sonoda,  
554 M., Firl, A., McNeilage, M.A., Douglas, M.J., Wang, T., et al. (2019). Two  
555 Y-chromosome-encoded genes determine sex in kiwifruit. *Nature plants*  
556 5:801-809.
- 557 Bachtrog, D. (2013). Y-chromosome evolution: emerging insights into processes of  
558 Y-chromosome degeneration. *Nature reviews Genetics* 14:113-124.
- 559 Bawa, K.S. (1980). Evolution of Dioecy in Flowering Plants. *Annual Review of*  
560 *Ecology and Systematics* 11:15-39.
- 561 Bennett, T., van den Toorn, A., Sanchez-Perez, G.F., Campilho, A., Willemsen, V.,  
562 Snel, B., and Scheres, B. (2010). SOMBRERO, BEARSKIN1, and BEARSKIN2  
563 regulate root cap maturation in *Arabidopsis*. *The Plant cell* 22:640-654.
- 564 Bergero, R., and Charlesworth, D. (2009). The evolution of restricted recombination  
565 in sex chromosomes. *Trends in ecology & evolution* 24:94-102.
- 566 Brautigam, K., Soolanayakanahally, R., Champigny, M., Mansfield, S., Douglas, C.,  
567 Campbell, M.M., and Cronk, Q. (2017). Sexual epigenetics: gender-specific  
568 methylation of a gene in the sex determining region of *Populus balsamifera*.  
569 *Scientific reports* 7:45388.
- 570 Chae, E., Bomblies, K., Kim, S.T., Karelina, D., Zaidem, M., Ossowski, S.,  
571 Martin-Pizarro, C., Laitinen, R.A., Rowan, B.A., Tenenboim, H., et al. (2014).  
572 Species-wide genetic incompatibility analysis identifies immune genes as hot  
573 spots of deleterious epistasis. *Cell* 159:1341-1351.
- 574 Charlesworth, B. (1991). The evolution of sex chromosomes. *Science* 251:1030-1033.
- 575 Charlesworth, B., and Charlesworth, D. (1978). A Model for the Evolution of Dioecy  
576 and Gynodioecy. *The American Naturalist* 112:975-997.
- 577 Charlesworth, D. (2012). Plant sex chromosome evolution. *Journal of Experimental*  
578 *Botany* 64:405-420.
- 579 Charlesworth, D. (2016). Plant Sex Chromosomes. *Annual Review of Plant Biology*  
580 67:397-420.
- 581 Chen, Y., Wang, T., Fang, L., Li, X., and Yin, T. (2016). Confirmation of Single-Locus  
582 Sex Determination and Female Heterogamety in Willow Based on Linkage  
583 Analysis. *PloS one* 11:e0147671.
- 584 Chen, Z., Ai, F., Zhang, J., Ma, X., Yang, W., Wang, W., Su, Y., Wang, M., Yang, Y.,  
585 Mao, K., et al. (2020) Survival in the Tropics despite isolation, inbreeding and  
586 asexual reproduction: insights from the genome of the world's southernmost  
587 poplar (*Populus ilicifolia*). *The Plant Journal* doi:10.1111/tpj.14744.



- 588 Dai, X., Hu, Q., Cai, Q., Feng, K., Ye, N., Tuskan, G.A., Milne, R., Chen, Y., Wan, Z.,  
589 Wang, Z., et al. (2014). The willow genome and divergent evolution from poplar  
590 after the common genome duplication. *Cell Research* 24:1274-1277.
- 591 DePristo, M.A., Banks, E., Poplin, R., Garimella, K.V., Maguire, J.R., Hartl, C.,  
592 Philippakis, A.A., del Angel, G., Rivas, M.A., Hanna, M., et al. (2011). A  
593 framework for variation discovery and genotyping using next-generation DNA  
594 sequencing data. *Nature genetics* 43:491-498.
- 595 Feng, G., Sanderson, B.J., Keefover-Ring, K., Liu, J., Ma, T., Yin, T., Smart, L.B.,  
596 DiFazio, S.P., and Olson, M.S. (2020). Pathways to sex determination in plants:  
597 how many roads lead to Rome? *Current Opinion in Plant Biology* 54:61-68.
- 598 Gaudet, M., Jorge, V., Paolucci, I., Beritognolo, I., Mugnozza, G.S., and Sabatti, M.  
599 (2008). Genetic linkage maps of *Populus nigra* L. including AFLPs, SSRs, SNPs,  
600 and sex trait. *Tree Genetics & Genomes* 4:25-36.
- 601 Geraldès, A., Hefer, C.A., Capron, A., Kolosova, N., Martínez-Nuñez, F.,  
602 Soolanayakanahally, R.Y., Stanton, B., Guy, R.D., Mansfield, S.D., Douglas, C.J.,  
603 et al. (2015). Recent Y chromosome divergence despite ancient origin of dioecy  
604 in poplars (*Populus*). *Molecular Ecology* 24:3243-3256.
- 605 Gong, L., Wong, C.H., Idol, J., Ngan, C.Y., and Wei, C.L. (2019). Ultra-long Read  
606 Sequencing for Whole Genomic DNA Analysis. *Journal of visualized*  
607 *experiments: JoVE*. 10.3791/58954.
- 608 Han, Y., and Jiao, Y. (2015). APETALA1 establishes determinate floral meristem  
609 through regulating cytokinins homeostasis in *Arabidopsis*. *Plant signaling &*  
610 *behavior* 10:e989039.
- 611 Harkess, A., Zhou, J., Xu, C., Bowers, J.E., Van der Hulst, R., Ayyampalayam, S.,  
612 Mercati, F., Riccardi, P., McKain, M.R., Kakrana, A., et al. (2017). The  
613 asparagus genome sheds light on the origin and evolution of a young Y  
614 chromosome. *Nature communications* 8:1279.
- 615 Henry, I.M., Akagi, T., Tao, R., and Comai, L. (2018). One Hundred Ways to Invent  
616 the Sexes: Theoretical and Observed Paths to Dioecy in Plants. *Annual Review*  
617 *of Plant Biology* 69:553-575.
- 618 Hobza, R., Cegan, R., Jesionek, W., Kejnovsky, E., Vyskot, B., and Kubat, Z. (2017).  
619 Impact of repetitive elements on the Y chromosome formation in plants. *Genes*  
620 8:302.
- 621 Hobza, R., Kubat, Z., Cegan, R., Jesionek, W., Vyskot, B., and Kejnovsky, E. (2015).  
622 Impact of repetitive DNA on sex chromosome evolution in plants. *Chromosome*  
623 *Research* 23:561-570.
- 624 Hou, J., Ye, N., Zhang, D., Chen, Y., Fang, L., Dai, X., and Yin, T. (2015). Different  
625 autosomes evolved into sex chromosomes in the sister genera of *Salix* and  
626 *Populus*. *Scientific reports* 5:9076.
- 627 Hu, H., Yang, W., Zheng, Z., Niu, Z., Yang, Y., Wan, D., Liu, J., and Ma, T. (2020).  
628 Analysis of Alternative Splicing and Alternative Polyadenylation in *Populus alba*  
629 var. *pyramidalis* by Single-Molecular Long-Read Sequencing. *Frontiers in*  
630 *genetics* 11:48.
- 631 Jain, M., Koren, S., Miga, K.H., Quick, J., Rand, A.C., Sasani, T.A., Tyson, J.R.,

- 632 Beggs, A.D., Dilthey, A.T., Fiddes, I.T., et al. (2018). Nanopore sequencing and  
633 assembly of a human genome with ultra-long reads. *Nature Biotechnology*  
634 36:338-345.
- 635 Kapitonov, V.V., and Jurka, J. (2007). Helitrons on a roll: eukaryotic rolling-circle  
636 transposons. *Trends in genetics: TIG* 23:521-529.
- 637 Kersten, B., Pakull, B., Groppe, K., Lueneburg, J., and Fladung, M. (2014). The  
638 sex-linked region in *Populus tremuloides* Turesson 141 corresponds to a  
639 pericentromeric region of about two million base pairs on *P. trichocarpa*  
640 chromosome 19. *Plant biology* 16:411-418.
- 641 Khan, A., Garbelli, A., Grossi, S., Florentin, A., Batelli, G., Acuna, T., Zolla, G., Kaye,  
642 Y., Paul, L.K., Zhu, J.K., et al. (2014). The *Arabidopsis* STRESS RESPONSE  
643 SUPPRESSOR DEAD-box RNA helicases are nucleolar- and  
644 chromocenter-localized proteins that undergo stress-mediated relocalization and  
645 are involved in epigenetic gene silencing. *The Plant journal* 79:28-43.
- 646 Kieber, J.J., and Schaller, G.E. (2018). Cytokinin signaling in plant development.  
647 *Development* 145.
- 648 Kielbasa, S.M., Wan, R., Sato, K., Horton, P., and Frith, M.C. (2011). Adaptive seeds  
649 tame genomic sequence comparison. *Genome research* 21:487-493.
- 650 Koren, S., Walenz, B.P., Berlin, K., Miller, J.R., Bergman, N.H., and Phillippy, A.M.  
651 (2017). Canu: scalable and accurate long-read assembly via adaptive k-mer  
652 weighting and repeat separation. *Genome research* 27:722-736.
- 653 Kuroha, T., Tokunaga, H., Kojima, M., Ueda, N., Ishida, T., Nagawa, S., Fukuda, H.,  
654 Sugimoto, K., and Sakakibara, H. (2009). Functional analyses of LONELY GUY  
655 cytokinin-activating enzymes reveal the importance of the direct activation  
656 pathway in *Arabidopsis*. *The Plant cell* 21:3152-3169.
- 657 Li, H. (2018). Minimap2: pairwise alignment for nucleotide sequences.  
658 *Bioinformatics* 34:3094-3100.
- 659 Li, H., and Durbin, R. (2009). Fast and accurate short read alignment with  
660 Burrows-Wheeler transform. *Bioinformatics* 25:1754-1760.
- 661 Li, H., Handsaker, B., Wysoker, A., Fennell, T., Ruan, J., Homer, N., Marth, G.,  
662 Abecasis, G., and Durbin, R. (2009). The Sequence Alignment/Map format and  
663 SAMtools. *Bioinformatics* 25:2078-2079.
- 664 Li, M., Wang, D., Zhang, L., Kang, M., Lu, Z., Zhu, R., Mao, X., Xi, Z., and Ma, T.  
665 (2019). Intergeneric Relationships within the Family Salicaceae *s.l.* Based on  
666 Plastid Phylogenomics. *International journal of molecular sciences* 20:3788.
- 667 Ma, J., Wan, D., Duan, B., Bai, X., Bai, Q., Chen, N., and Ma, T. (2019). Genome  
668 sequence and genetic transformation of a widely distributed and cultivated poplar.  
669 *Plant biotechnology journal* 17:451-460.
- 670 Ma, T., Wang, K., Hu, Q., Xi, Z., Wan, D., Wang, Q., Feng, J., Jiang, D., Ahani, H.,  
671 Abbott, R.J., et al. (2018). Ancient polymorphisms and divergence hitchhiking  
672 contribute to genomic islands of divergence within a poplar species complex.  
673 *Proceedings of the National Academy of Sciences of the United States of*  
674 *America* 115:E236-e243.
- 675 Melnikova, N.V., Kudryavtseva, A.V., Borkhert, E.V., Pushkova, E.N., Fedorova,

- 676 M.S., Snezhkina, A.V., Krasnov, G.S., and Dmitriev, A.A. (2019). Sex-specific  
677 polymorphism of *MET1* and *ARR17* genes in *Populus × sibirica*. *Biochimie*  
678 162:26-32.
- 679 Ming, R., Bendahmane, A., and Renner, S.S. (2011). Sex chromosomes in land plants.  
680 *Annual Review of Plant Biology* 62:485-514.
- 681 Mitsuda, N., Seki, M., Shinozaki, K., and Ohme-Takagi, M. (2005). The NAC  
682 transcription factors NST1 and NST2 of *Arabidopsis* regulate secondary wall  
683 thickenings and are required for anther dehiscence. *The Plant cell* 17:2993-3006.
- 684 Morgante, M., Brunner, S., Pea, G., Fengler, K., Zuccolo, A., and Rafalski, A. (2005).  
685 Gene duplication and exon shuffling by helitron-like transposons generate  
686 intraspecies diversity in maize. *Nature genetics* 37:997-1002.
- 687 Pakull, B., Groppe, K., Meyer, M., Markussen, T., and Fladung, M. (2009). Genetic  
688 linkage mapping in aspen (*Populus tremula* L. and *Populus tremuloides* Michx.).  
689 *Tree Genetics & Genomes* 5:505-515.
- 690 Pakull, B., Kersten, B., Lüneburg, J., and Fladung, M. (2015). A simple PCR-based  
691 marker to determine sex in aspen. *Plant biology* 17:256-261.
- 692 Palmer, D.H., Rogers, T.F., Dean, R., and Wright, A.E. (2019). How to identify sex  
693 chromosomes and their turnover. *Molecular Ecology* 28:4709-4724.
- 694 Paolucci, I., Gaudet, M., Jorge, V., Beritognolo, I., Terzoli, S., Kuzminsky, E., Muleo,  
695 R., Scarascia Mugnozza, G., and Sabatti, M. (2010). Genetic linkage maps of  
696 *Populus alba* L. and comparative mapping analysis of sex determination across  
697 *Populus* species. *Tree Genetics & Genomes* 6:863-875.
- 698 Peto, F. (2011). Cytology of poplar species and natural hybrids. *Canadian Journal of*  
699 *Research* 16:445-455.
- 700 Pucholt, P., Rönnerberg-Wästljung, A.C., and Berlin, S. (2015). Single locus sex  
701 determination and female heterogamety in the basket willow (*Salix viminalis* L.).  
702 *Heredity* 114:575-583.
- 703 Pucholt, P., Wright, A.E., Conze, L.L., Mank, J.E., and Berlin, S. (2017). Recent Sex  
704 Chromosome Divergence despite Ancient Dioecy in the Willow *Salix viminalis*.  
705 *Molecular Biology and Evolution* 34:1991-2001.
- 706 Purcell, S., Neale, B., Todd-Brown, K., Thomas, L., Ferreira, M.A., Bender, D.,  
707 Maller, J., Sklar, P., de Bakker, P.I., Daly, M.J., et al. (2007). PLINK: a tool set  
708 for whole-genome association and population-based linkage analyses. *American*  
709 *journal of human genetics* 81:559-575.
- 710 Renner, S.S. (2014). The relative and absolute frequencies of angiosperm sexual  
711 systems: dioecy, monoecy, gynodioecy, and an updated online database.  
712 *American journal of botany* 101:1588-1596.
- 713 Renner, S.S., and Ricklefs, R.E. (1995). Dioecy and its correlates in the flowering  
714 plants. *American journal of botany*:596-606.
- 715 Sanderson, B., Feng, G., Hu, N., Grady, J., Carlson, C., Smart, B., Keefover-Ring, K.,  
716 Yin, T., Ma, T., Liu, J., DiFazio, S., et al. (2020). Sex determination through X-Y  
717 heterogamety in *Salix nigra*. *bioRxiv*.
- 718 Stanke, M., Keller, O., Gunduz, I., Hayes, A., Waack, S., and Morgenstern, B. (2006).  
719 AUGUSTUS: ab initio prediction of alternative transcripts. *Nucleic acids*

- 720 research 34:W435-439.
- 721 Tamura, K., Peterson, D., Peterson, N., Stecher, G., Nei, M., and Kumar, S. (2011).  
722 MEGA5: molecular evolutionary genetics analysis using maximum likelihood,  
723 evolutionary distance, and maximum parsimony methods. *Molecular Biology*  
724 *and Evolution* 28:2731-2739.
- 725 Tarailo-Graovac, M., and Chen, N. (2009). Using RepeatMasker to identify repetitive  
726 elements in genomic sequences. *Current protocols in bioinformatics* Chapter  
727 4:Unit 4.10.
- 728 Tennessen, J.A., Wei, N., Straub, S.C.K., Govindarajulu, R., Liston, A., and Ashman,  
729 T.L. (2018). Repeated translocation of a gene cassette drives sex-chromosome  
730 turnover in strawberries. *PLoS biology* 16:e2006062.
- 731 Thévenin, J., Pollet, B., Letarnec, B., Saulnier, L., Gissot, L., Maia-Grondard, A.,  
732 Lapierre, C., and Jouanin, L. (2011). The simultaneous repression of CCR and  
733 CAD, two enzymes of the lignin biosynthetic pathway, results in sterility and  
734 dwarfism in *Arabidopsis thaliana*. *Molecular plant* 4:70-82.
- 735 Tokunaga, H., Kojima, M., Kuroha, T., Ishida, T., Sugimoto, K., Kiba, T., and  
736 Sakakibara, H. (2012). *Arabidopsis* lonely guy (LOG) multiple mutants reveal a  
737 central role of the LOG-dependent pathway in cytokinin activation. *The Plant*  
738 *journal*: 69:355-365.
- 739 Torres, M.F., Mathew, L.S., Ahmed, I., Al-Azwani, I.K., Krueger, R., Rivera-Nuñez,  
740 D., Mohamoud, Y.A., Clark, A.G., Suhre, K., and Malek, J.A. (2018).  
741 Genus-wide sequencing supports a two-locus model for sex-determination in  
742 *Phoenix*. *Nature communications* 9:3969.
- 743 Tuskan, G.A., and Difazio, S., and Jansson, S., and Bohlmann, J., and Grigoriev, I.,  
744 and Hellsten, U., and Putnam, N., and Ralph, S., and Rombauts, S., and Salamov,  
745 A., et al. (2006). The genome of black cottonwood, *Populus trichocarpa* (Torr. &  
746 Gray). *Science* 313:1596-1604.
- 747 Wang, J., Na, J.K., Yu, Q., Gschwend, A.R., Han, J., Zeng, F., Aryal, R., VanBuren, R.,  
748 Murray, J.E., Zhang, W., et al. (2012). Sequencing papaya X and Y<sup>h</sup>  
749 chromosomes reveals molecular basis of incipient sex chromosome evolution.  
750 *Proceedings of the National Academy of Sciences of the United States of*  
751 *America* 109:13710-13715.
- 752 Wang, M., Zhang, L., Zhang, Z., Li, M., Wang, D., Zhang, X., Xi, Z., Keefover-Ring,  
753 K., Smart, L.B., DiFazio, S.P., et al. (2020). Phylogenomics of the genus *Populus*  
754 reveals extensive interspecific gene flow and balancing selection. *The New*  
755 *phytologist* 225:1370-1382.
- 756 Wybouw, B., and De Rybel, B. (2019). Cytokinin - A Developing Story. *Trends in*  
757 *plant science* 24:177-185.
- 758 Xue, L., Wu, H., Chen, Y., Li, X., Hou, J., Lu, J., Wei, S., Dai, X., Olson, M., Liu, J.  
759 (2020). Two antagonistic effect genes mediate separation of sexes in a fully  
760 dioecious plant. *bioRxiv*.
- 761 Yang, W., Wang, K., Zhang, J., Ma, J., Liu, J., and Ma, T. (2017). The draft genome  
762 sequence of a desert tree *Populus pruinosa*. *GigaScience* 6:1-7.
- 763 Yang, Y., Ma, T., Wang, Z., Lu, Z., Li, Y., Fu, C., Chen, X., Zhao, M., Olson, M.S.,

- 764 and Liu, J. (2018). Genomic effects of population collapse in a critically  
765 endangered ironwood tree *Ostrya rehderiana*. *Nature communications* 9:5449.
- 766 Yin, T., Difazio, S.P., Gunter, L.E., Zhang, X., Sewell, M.M., Woolbright, S.A., Allan,  
767 G.J., Kelleher, C.T., Douglas, C.J., Wang, M., et al. (2008). Genome structure  
768 and emerging evidence of an incipient sex chromosome in *Populus*. *Genome*  
769 *research* 18:422-430.
- 770 Zhang, J., Boualem, A., Bendahmane, A., and Ming, R. (2014). Genomics of sex  
771 determination. *Current Opinion in Plant Biology* 18:110-116.
- 772 Zhang, L., Xi, Z., Wang, M., Guo, X., and Ma, T. (2018). Plastome phylogeny and  
773 lineage diversification of Salicaceae with focus on poplars and willows. *Ecology*  
774 *and evolution* 8:7817-7823.
- 775 Zhang, Z., Chen, Y., Zhang, J., Ma, X., Li, Y., Li, M., Wang, D., Kang, M., Wu, H.,  
776 Yang, Y., et al. (2020). Improved genome assembly provides new insights into  
777 genome evolution in a desert poplar (*Populus euphratica*). *Molecular ecology*  
778 *resources*.
- 779 Zhou, R., Macaya-Sanz, D., Carlson, C.H., Schmutz, J., Jenkins, J.W., Kudrna, D.,  
780 Sharma, A., Sandor, L., Shu, S., Barry, K., et al. (2020). A willow sex  
781 chromosome reveals convergent evolution of complex palindromic repeats.  
782 *Genome biology* 21:38.
- 783 Zhou, R., Macaya-Sanz, D., Rodgers-Melnick, E., Carlson, C.H., Gouker, F.E., Evans,  
784 L.M., Schmutz, J., Jenkins, J.W., Yan, J., Tuskan, G.A., et al. (2018).  
785 Characterization of a large sex determination region in *Salix purpurea* L.  
786 (Salicaceae). *Molecular genetics and genomics: MGG* 293:1437-1452.
- 787  
788  
789

790 **Figure Legends**

791

792 **Fig. 1 XY sex determination on chromosome 14 in *P. euphratica*.** (A) Manhattan  
793 plot of *P. euphratica* based on the results of genome-wide association study (GWAS)  
794 with the male genome as reference. The y-axis represents the strength of association  
795 ( $-\log_{10}(P \text{ value})$ ) for each SNP sorted by chromosomes and scaffolds (SC; x-axis).  
796 The red line indicates the significance after Bonferroni multiple corrections ( $\alpha < 0.05$ ).  
797 Note that the scaffold '001598F' is located on chromosome 14 based on its syntenic  
798 relationship with the proximal end of chromosome 14 of *P. trichocarpa*. (B) Summary  
799 of male *P. euphratica* genome regions containing SNPs significantly associated with  
800 sex. SNP\*, significantly associated SNPs; Homo, Homozygous; Hete, Heterozygosis.  
801 (C) Synteny relationships between our assembled Y-contig and X chromosome of *P.*  
802 *euphratica*, as well as the corresponding region of chromosome 14 for *P. alba*, *P.*  
803 *trichocarpa* and *S. purpurea*. The highlighted part represents the sex determination  
804 region (SDR), yellow for Y-SDR and green for X-SDR. Schematic diagram showing  
805 the corresponding position of the SDR on chromosome 14 of *P. euphratica*. (D)  
806 Phylogenetic relationships of the homolog pairs (HP) shared between Y- and X-SDR  
807 of *P. euphratica* and their orthologous genes in other Salicaceae species. Detailed  
808 information about these genes is listed in Table S7 and additional phylogenetic trees  
809 are shown in Fig. S7. Note that only the orthologous genes located on the  
810 corresponding region of chromosome 14 were used for phylogenetic analysis.

811

812

813 **Fig. 2 ZW sex determination on chromosome 19 in *P. alba*.** (A) Manhattan plot of *P.*  
814 *alba* based on the results of GWAS with female genome as reference respectively. The  
815 y-axis represents the strength of association ( $-\log_{10}(P \text{ value})$ ) for each SNP sorted by  
816 chromosomes and scaffolds (SC; x-axis). The red line indicates the significance after  
817 Bonferroni multiple corrections ( $\alpha < 0.05$ ). (B) Summary of female *P. alba* genome  
818 regions containing SNPs significantly associated with sex. SNP\*, significantly  
819 associated SNPs; Homo, Homozygous; Hete, Heterozygosis. (C) Synteny



820 relationships between our assembled W-contig and Z chromosome of *P. alba*, as well  
821 as the corresponding region of chromosome 19 for *P. euphratica*, *P. trichocarpa* and *S.*  
822 *purpurea*. The highlighted part represents SDR, red for W-SDR and blue for Z-SDR.  
823 Schematic diagram showing the corresponding position of the SDR on chromosome  
824 19 of *P. alba*. **(D)** Phylogenetic relationships of the homolog pairs (HP) shared  
825 between W- and Z-SDR of *P. alba* and their orthologous genes in other Salicaceae  
826 species. The detail information of these genes is listed in Table S12. Note that there  
827 are 3 copies for ‘HP2’ on the W-SDR of *P. alba*, and only the orthologous genes  
828 located on the corresponding region of chromosome 19 were used for phylogenetic  
829 analysis.

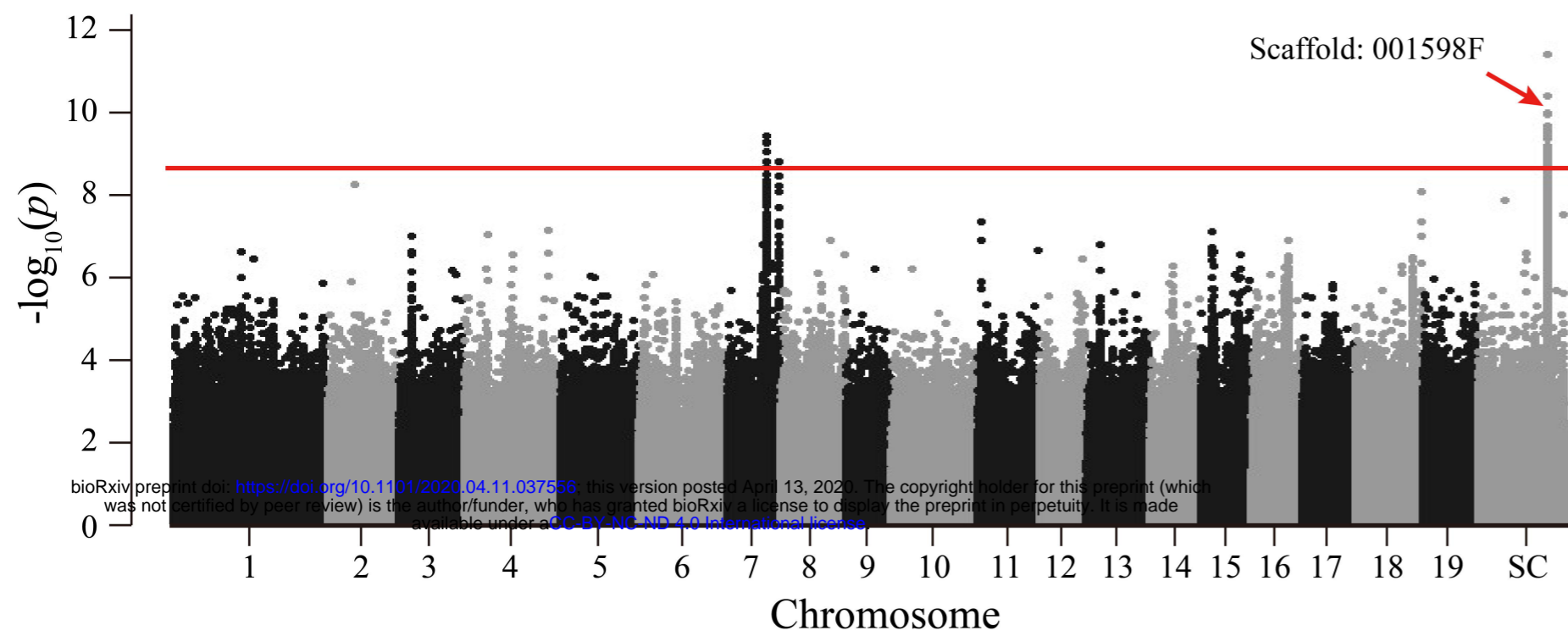
830

831 **Fig. 3 Evidence for SDR turnover in Salicaceae.** **(A)** Synteny relationships among  
832 the Y-SDR of *P. euphratica* (yellow) and the W-SDRs of *P. alba* (red) and *S. purpurea*  
833 (blue), showing the copies of *RR* intact gene (‘C’) and partial duplicates (‘S’: small  
834 duplicate; ‘L’: large duplicate) on their SDRs. For each species, corresponding  
835 positions for other *RR* gene copies or partial duplicates on the autosome are also  
836 shown. **(B)** Phylogenetic relationship of the *RR* sequences (including intact genes and  
837 partial duplicates) identified in the four species. The tree was rooted by a paralogous  
838 gene ‘*RR16*’. The gene structures and relative positions of *Helitron* and *Copia*-like  
839 LTR are also shown. Phylogenetic relationships of the *Helitron* **(C)** and *Copia*-like  
840 LTR **(D)** around the *RR* sequences. All the sequences were named according to Fig.  
841 3A. *Peu*: *P. euphratica*; *Pal*: *P. alba*; *Ptr*: *P. trichocarpa*; *Spur*: *S. purpurea*.

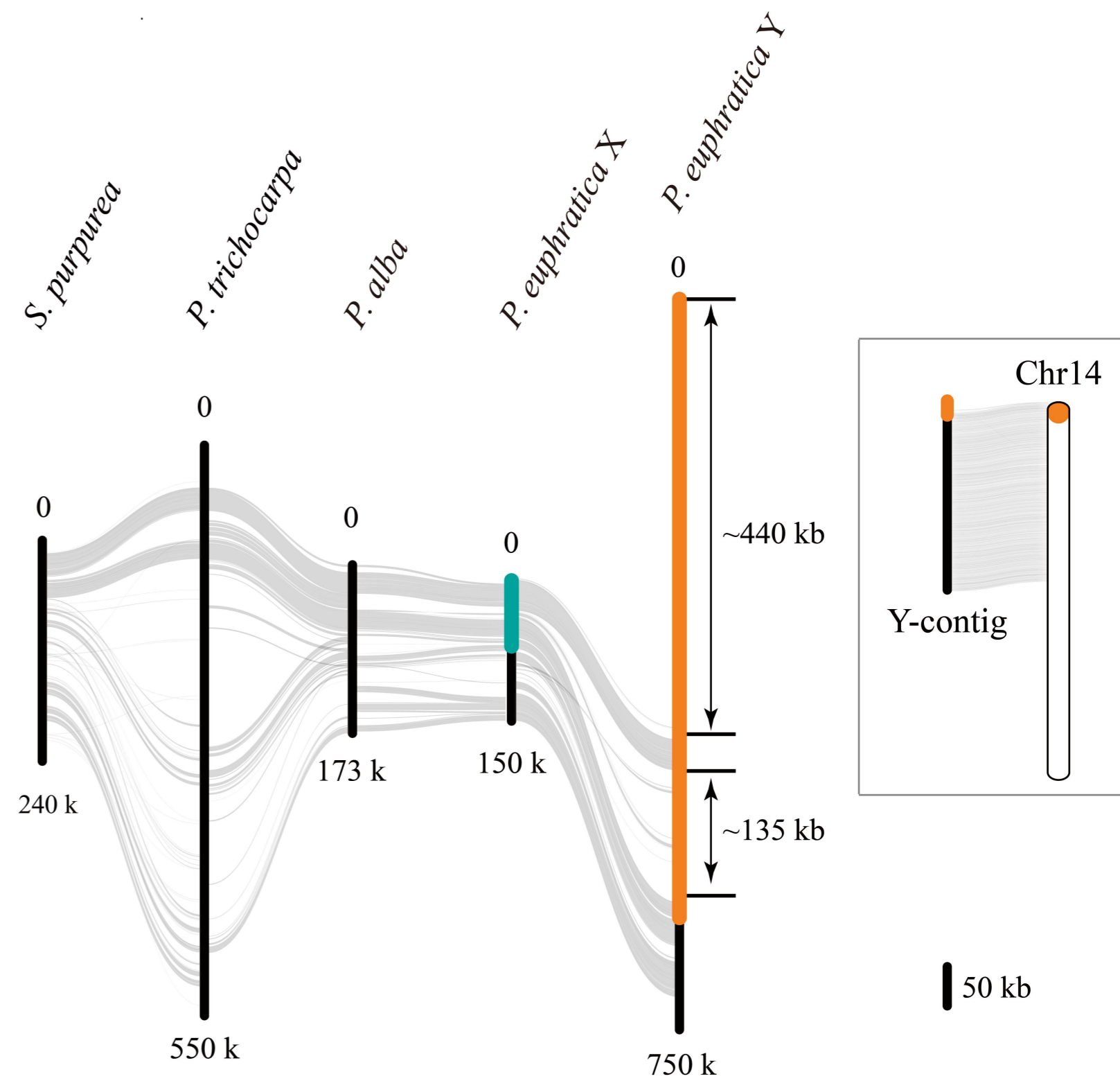
842

843 **Fig. 4 Hypothetical model for sex system turnovers in Salicaceae.** The W  
844 chromosomes of *P. alba* and *S. purpurea* both carry several intact *RR* genes and are  
845 likely to serve as a dominate promoter of female function. On the Y chromosome of *P.*  
846 *euphratica*, partial duplicates of the *RR* gene are like to serve as a female suppressor  
847 by encoding an siRNA that targets the intact *RR* gene through RNA-directed DNA  
848 methylation. Note that Y-SDR of *P. trichocarpa* has not yet been assembled, so  
849 whether a similar pattern should be found in this species remains to be confirmed.

A



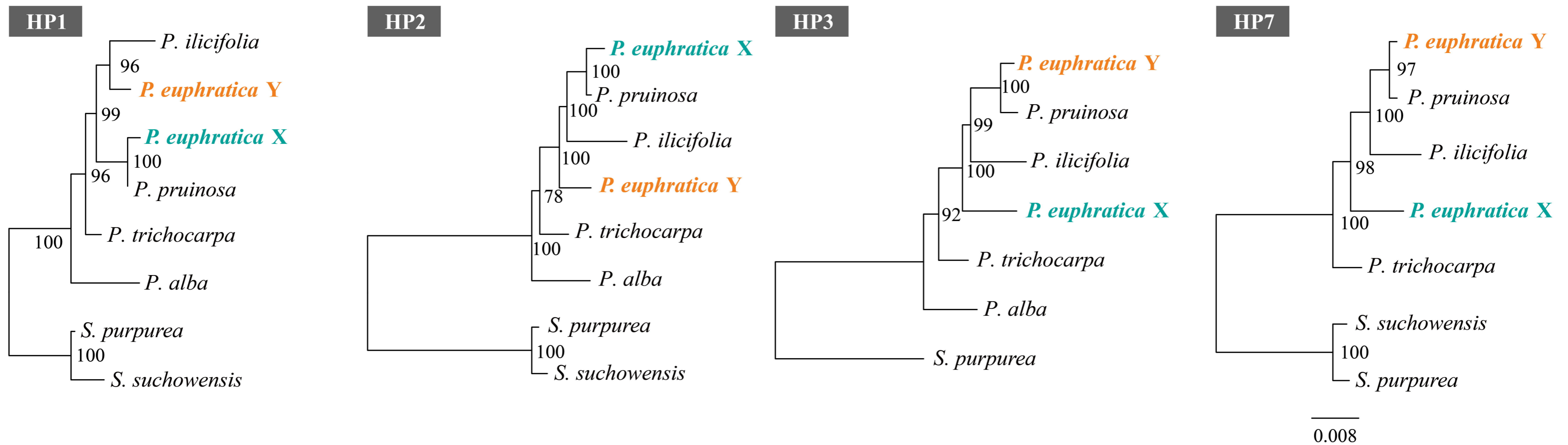
C



B

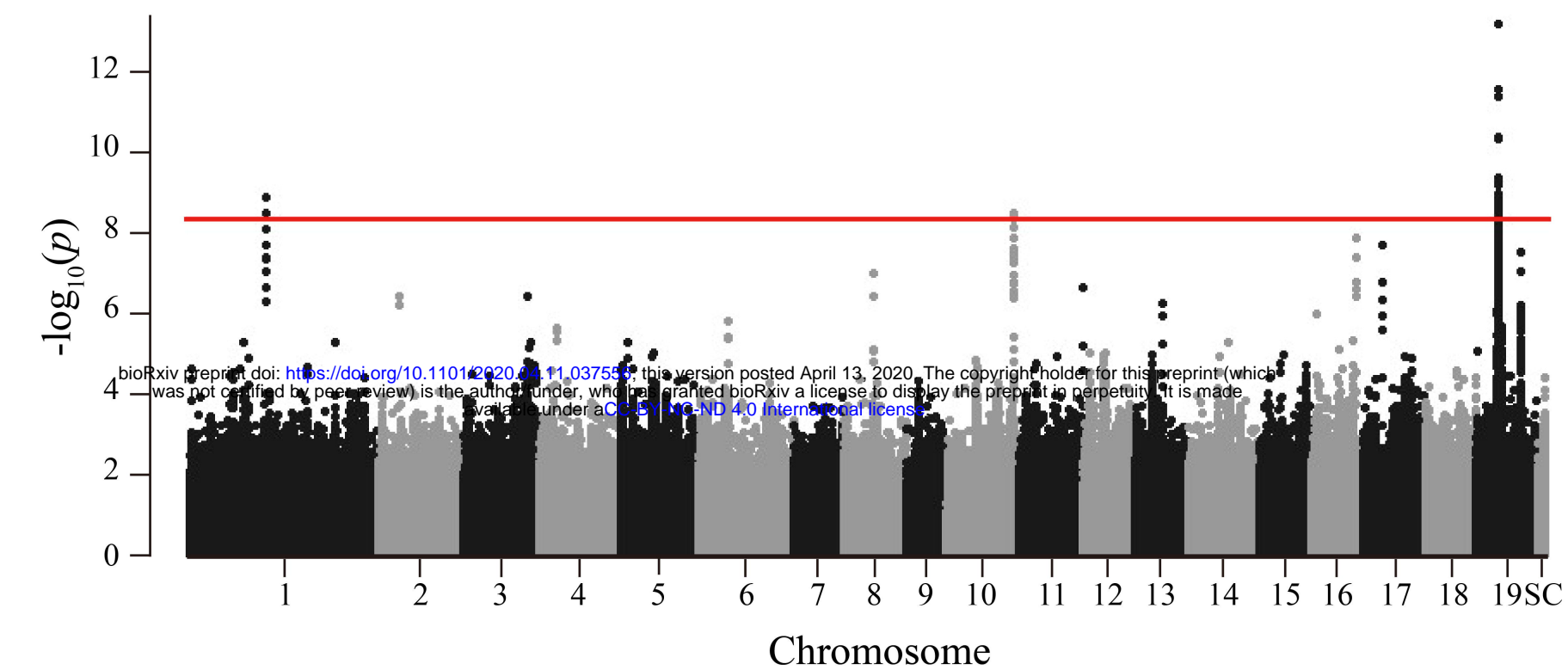
Reference genome	Scaffold ID	Chr ID	Position (bp)		SNP*	Female		Male	
			Start	End		Homo(%)	Hete(%)	Homo(%)	Heter(%)
	001598F	14	595	45,911	296	99.99	0.01	6.06	93.94
Male	Lachesis_group10	7	17,334,724	17,391,719	8	100.00	0.00	21.10	78.90
	Lachesis_group10	7	22,941,832	22,956,851	6	100.00	0.00	6.67	93.33
<b>Total</b>	-	-	-	-	<b>310</b>	<b>99.99</b>	<b>0.01</b>	<b>6.43</b>	<b>93.57</b>

D





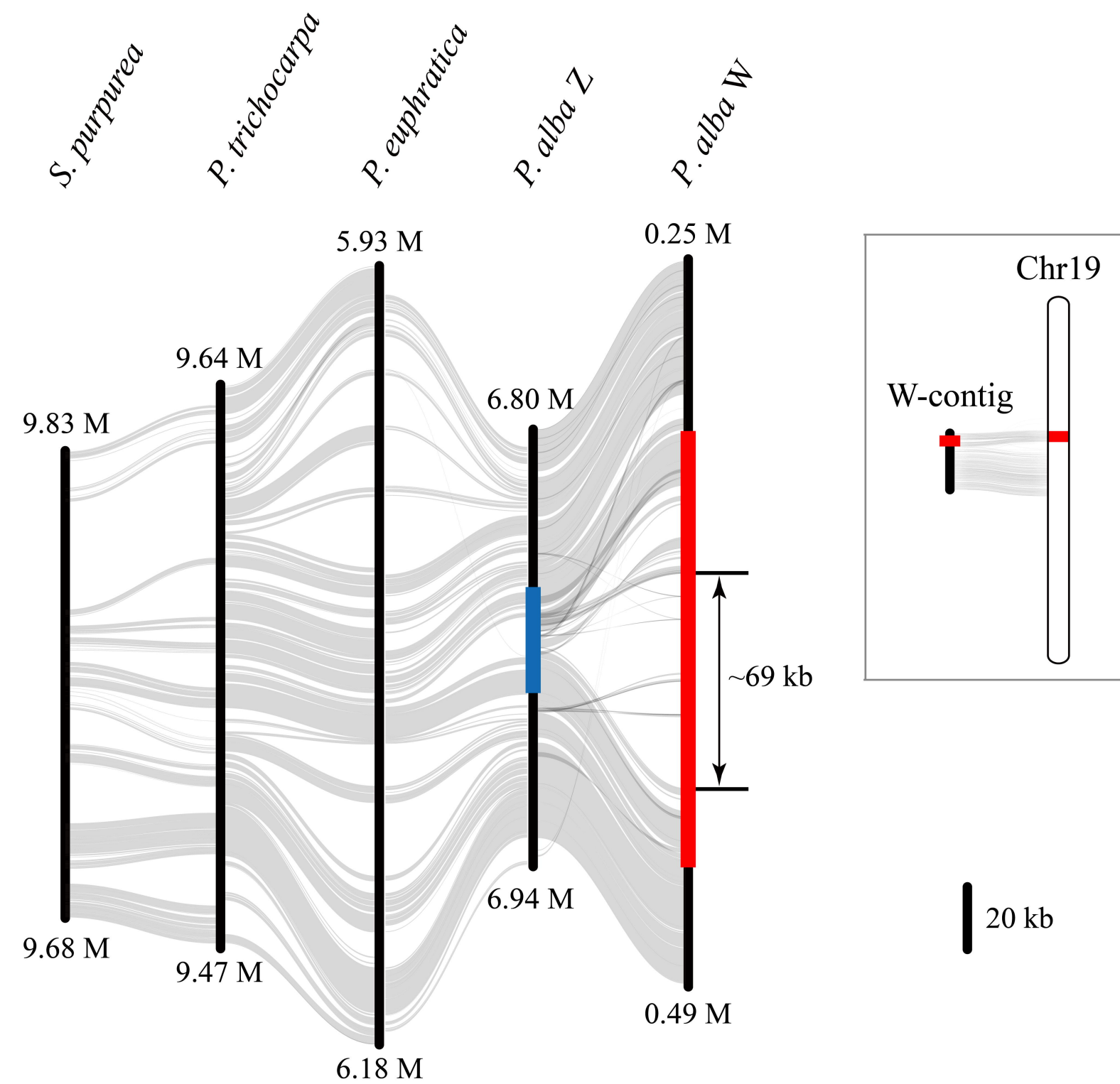
A



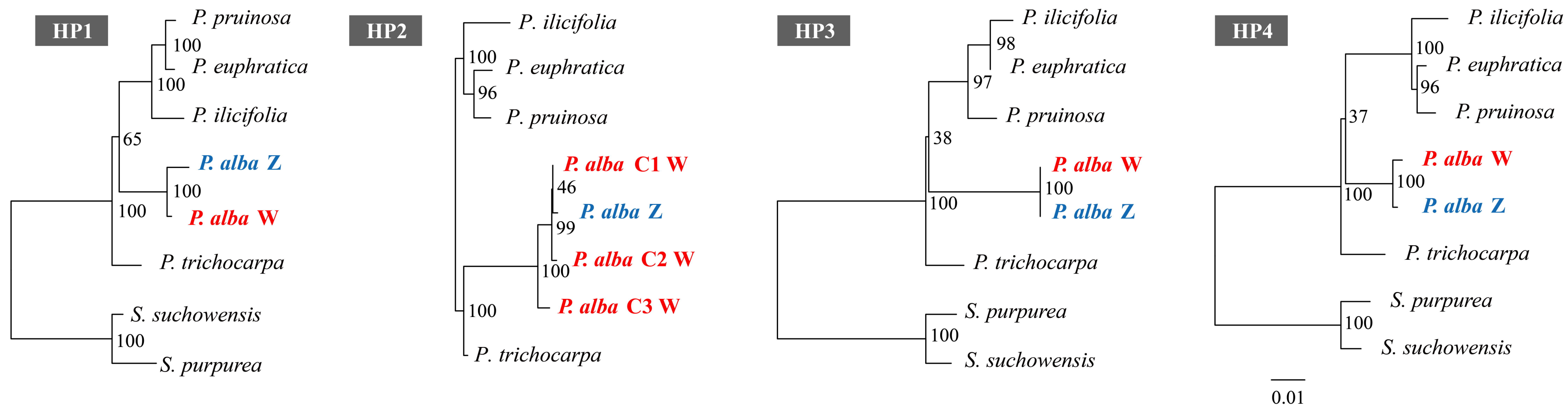
B

Reference genome	Scaffold ID	Chr ID	Position (bp)		SNP*	Female		Male	
			Start	End		Homo(%)	Hete(%)	Homo(%)	Hete(%)
	Contig42	19	317,074	440,815	48	8.44	91.56	96.61	3.39
<b>Female</b>	Contig111	10	131,470	132,638	4	6.67	93.33	96.08	3.92
	Contig319	1	26,758	26,805	3	2.23	97.78	96.67	3.33
	<b>Total</b>	-	-	-	<b>55</b>	<b>7.95</b>	<b>92.05</b>	<b>96.58</b>	<b>3.42</b>

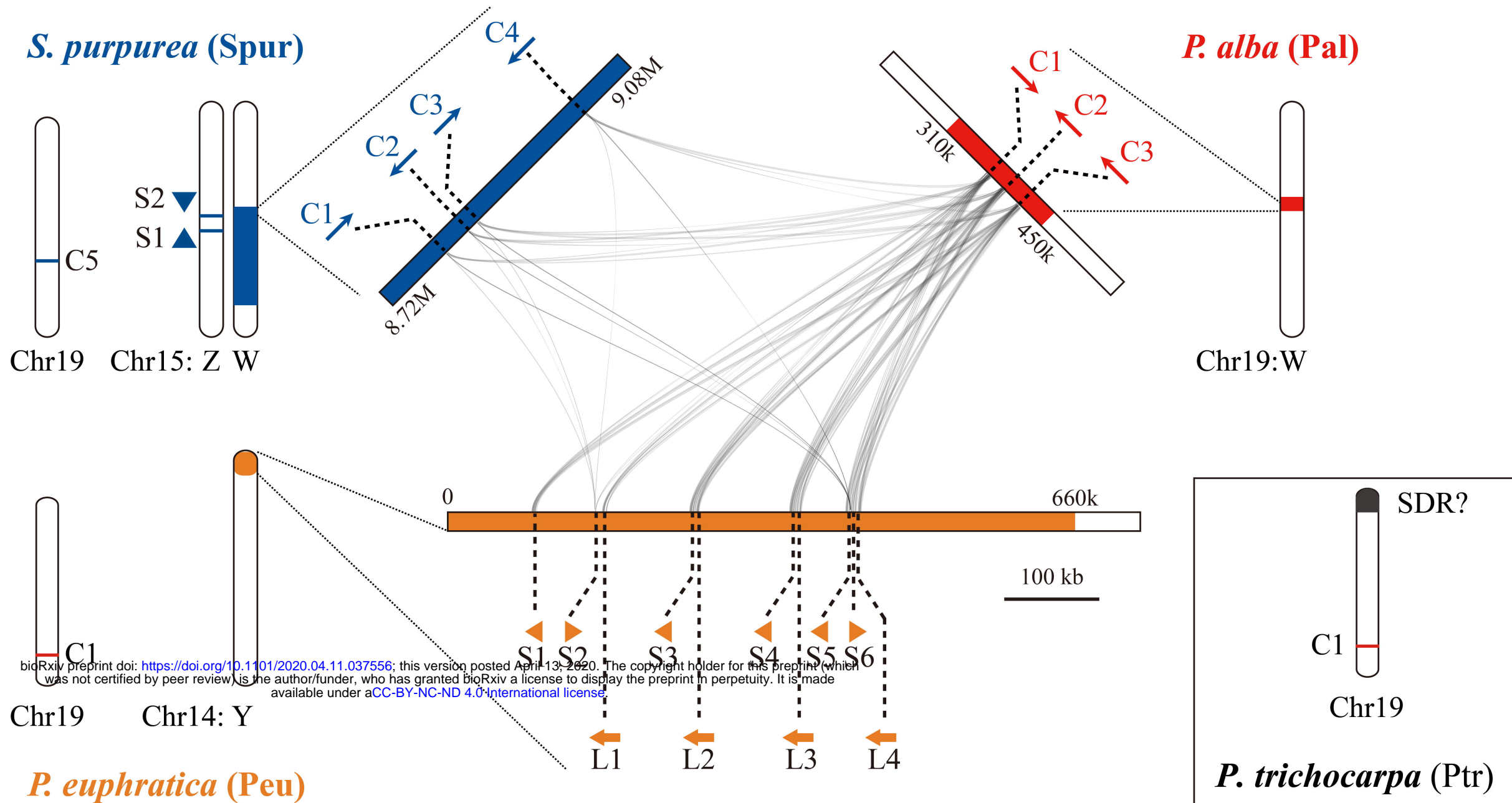
C



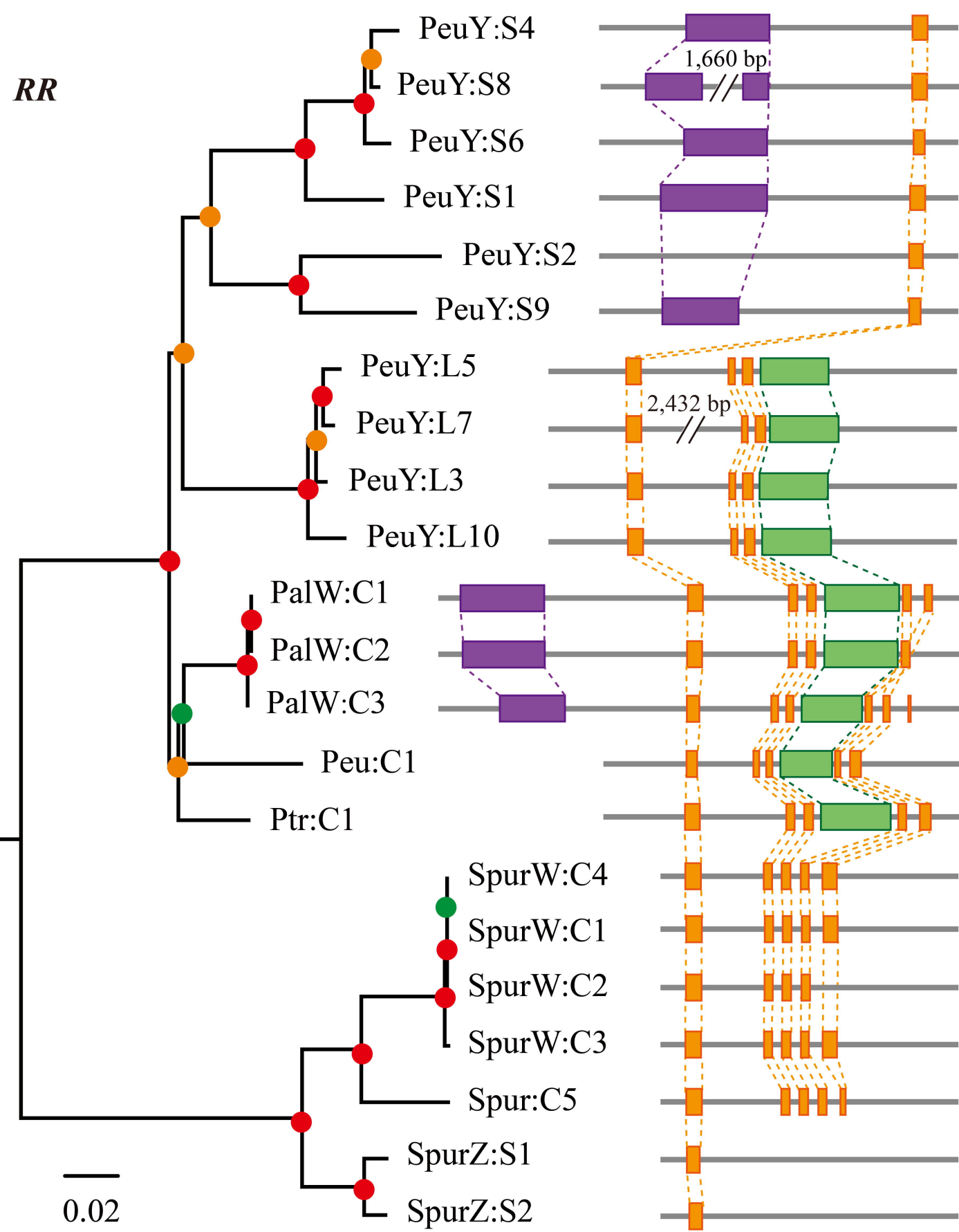
D



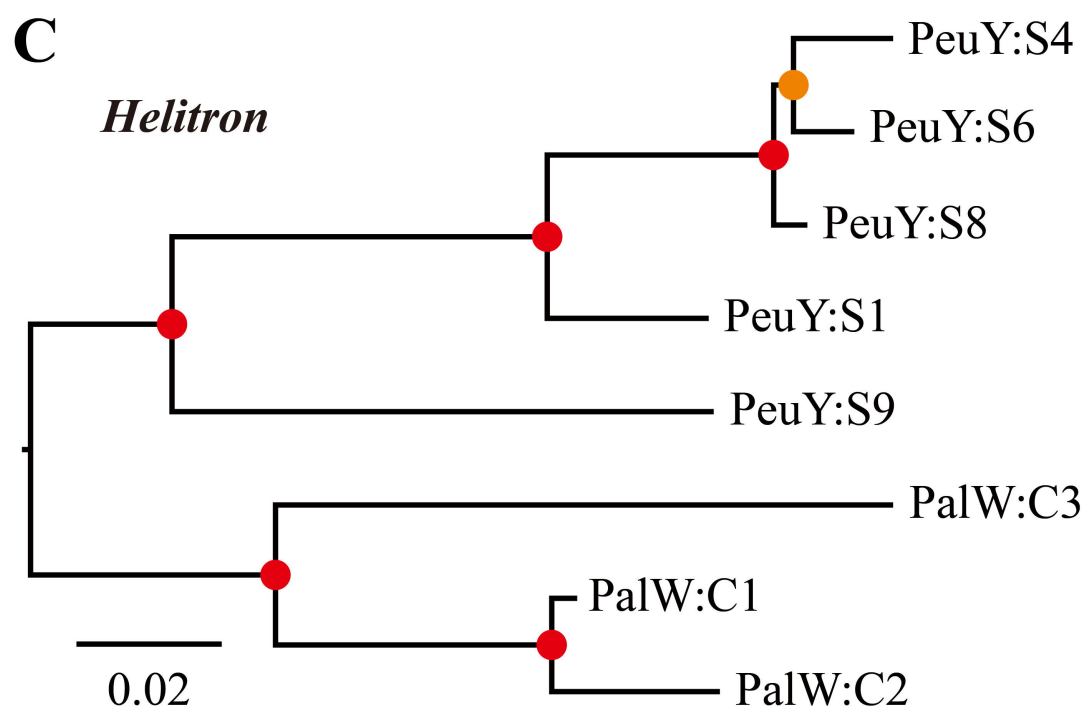
A



B



C



D

